

## **ANALYSIS OF MASONRY WALLS**

Masonry is a traditional construction material which has been used in housing as well as industrial structures for centuries. However, the mechanical response of masonry is quite complex, mainly because it is a composite material having a large number of possible modes of its failure. The mechanical response is further complicated due to a large variability in the mechanical properties of its constituents i.e. bricks and mortar. Furthermore, masonry characteristics are greatly influenced by the quality of workmanship, which is highly variable.

One of the most important tasks for engineers in masonry structures, either new to be constructed or old to be assessed for safety, is to determine the strength of masonry in different loading configurations. For normal steel or concrete structures, the strength of these materials is known from a series of tests. However, in the case of masonry, it is not possible to conduct meaningful tests on a scale that would represent 'masonry'. Moreover, it should be noted that the strength of masonry is required with bed joints in with different orientations, since masonry is an anisotropic material.

The strength of the constituents of masonry can, however, be determined by testing. For new construction bricks and mortar can be easily tested whilst for existing structures random samples can be obtained and tested albeit with some difficulty of dealing with small samples of mortar. Having established mechanical properties of the constituents, the engineer has to make some judgment regarding the strength of masonry in two orthogonal directions. Here the codes of practice may help but for complex structures, there is really no guidance, and more elaborate and sophisticated numerical approaches should be used.

It is very important, at the initial stage of analyzing any masonry structure, one of the tasks to be undertaken is to explore the possibility of developing a simple computational procedure (dubbed as Engineering Approach (EA) which could be used as a rough guide to check the structural behavior and validate the results obtained by any complex numerical analysis. A set of simplifying assumptions are made in the EA which are obviously different from those made in the more elaborate and sophisticated numerical approaches and one should not expect perfect matching of prediction of strength under various combinations of stress. Nevertheless, EA when fully developed in the form of bespoke stand-alone computer software could be a useful tool for the use of structural engineers engaged in masonry projects.

Assessment of the mechanical response of existing masonry buildings especially those likely to experience earthquake forces is a complex and challenging task. An earthquake can have a devastating effect in particular on unreinforced masonry structures. The analytical methods proposed by structural engineers for final analysis of masonry are often based on simplistic numerical procedures which cannot realistically address the seismic response of existing masonry structures or the new proposed systems of masonry structures without reinforced concrete walls or frames. The obtained results in some cases are misleading and not correct. This is primarily due to the fact that masonry is a complex composite material, which is anisotropic on the macro scale and has a large number of possible modes of failure. Thus, a rational approach to the problem should incorporate advanced nonlinear formulations that account for the diversity of mechanical characteristics.

Based on our experience, in evaluation of masonry structures, two among several approaches used in the past are briefly presented here (Gocevski 2007): (1) Engineering Approach and (2) The Critical Plane Approach.

### **1. Engineering Approach (EA)**

The assumptions made in the EA are essentially similar to those made in the multilaminate model for jointed rock masses [Zienkiewicz & Pande (1977); Pande, Beer & Williams (1990)]. Briefly, these are:

- a. Masonry consists of two sets of continuous and parallel joints.
- b. Bed joints have mechanical characteristics which are derived from that of mortar
- c. Head joints have mechanical characteristics which are derived from that of mortar and brick. Admittedly, the head joints are not continuous and if they are assumed to be so, appropriate shear strength based on the shear strength of brick material as well as mortar should be computed.
- d. The masonry can fail: failure on a bed joint or a head joint in tension or shear while brick units can also fail by cracking in tension based on the maximum principal stress criterion. More complicated failure criteria can be adopted for brick material but are out of scope for

this brief presentation.

A list of mechanical parameters required for the analysis is also given:

Item	Units	Brick	Mortar	
Internal friction <sup>1</sup> angle	°	55	43	
Cohesion <sup>1</sup>	kPa	2.38	0.176	
Tensile strength	kPa	1.0	0.07	
Elastic modulus	MPa	15,400	2200	
Poisson's ratio		0.2	0.3	
Length	mm	37.5		
Height	mm	12.5		
Thickness	mm	37.5	1.56	

<sup>1</sup> These parameters can be obtained from corresponding tensile and compressive strengths of bricks and mortar

They are based on the interpretation of information available for the experiments (of Samarsinghe & Hendry 1980). From the above data, the effective parameters for the 'equivalent' continuous head joints can be interpreted as follows:

Internal friction angle = 65.9°, Cohesion = 1.54 MPa, Tensile strength = 1.0 MPa

Based on the above parameters, failure stress is computed for various loading situations represented by the value of 'α', which is defined in figure below:

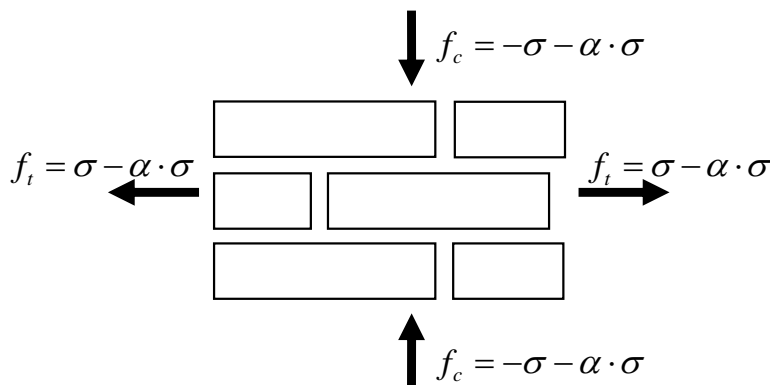


Fig.1 Definition of α (α = -1, 0, 1 represent uniaxial compression, pure shear and uniaxial tension respectively)

A value of stress which would cause failure on the bed or head joint for changing orientation of bed joint, is calculated, using linear Mohr-Coulomb criterion. Stresses are also calculated for each orientation in the brick material based on the anisotropic elastic properties of the masonry using principal stress failure criterion. The minimum value of stress which would cause failure in any constituent is picked up as the value for the corresponding orientation. Results are presented as a set of graphs showing 'normalised' failure stress against the orientation of the bed joint. The legend on the graphs is as follows:

- HD\_MC Failure of head joint in shear
- HD\_TC Failure of head joint in tension cut-off. The failure takes place in tension on a head joint and shearing of bed joints above and below the head joint
- BD\_MC Failure of bed joint in shear
- BD\_TC Failure of bed joint in tension cut-off
- Brick Tension failure takes place in the brick
- Exp Experimental tests [Samarsinghe & Hendry (1980)]
- ENG Engineering Approach

Variation of strength in tension and compression with the angle made by the bed joint to the horizontal line for

a specific set of mechanical parameters of constituents is presented below. Here comparison is also made with the test results of Samarsinghe & Hendry (1980).

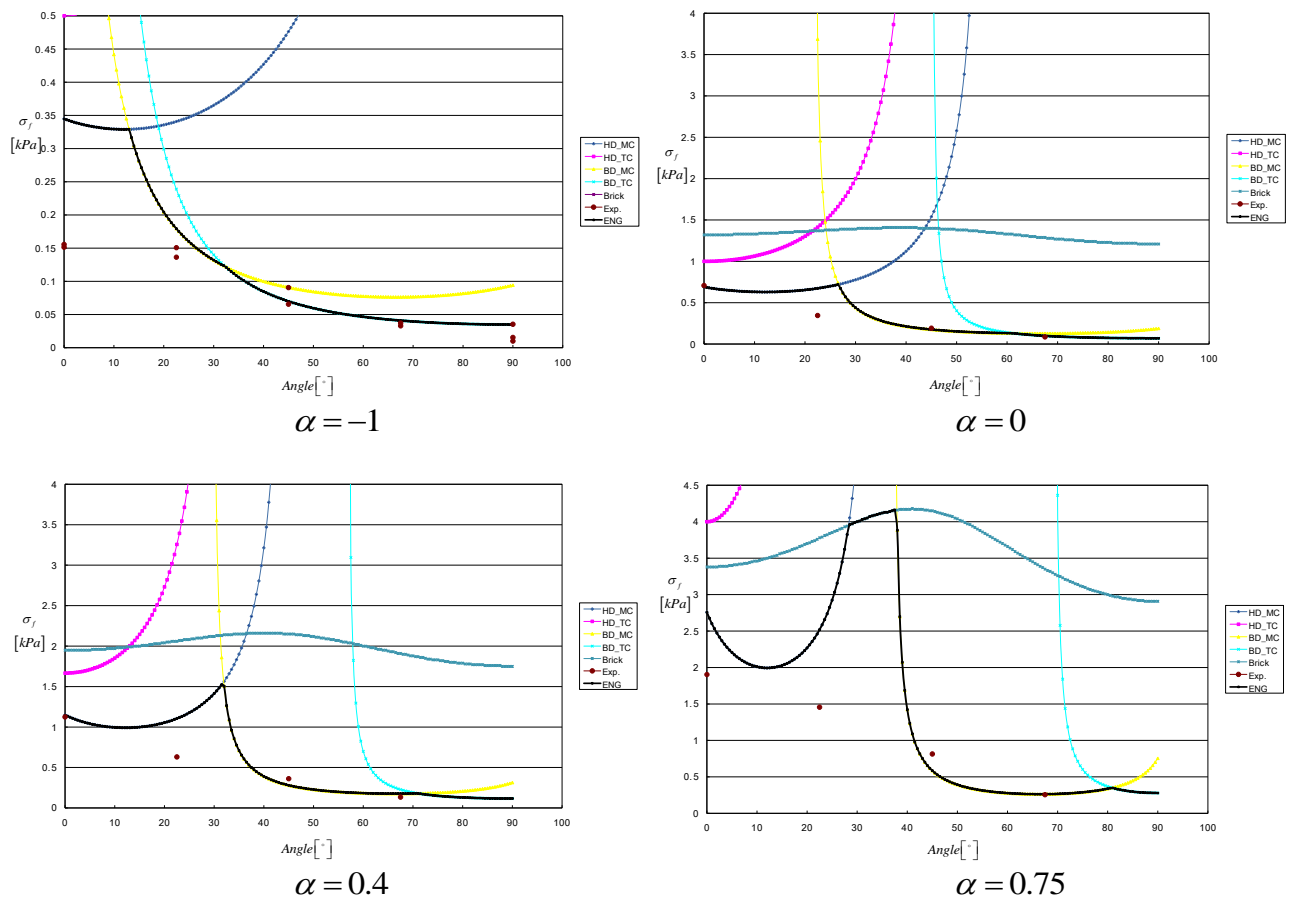


Fig. 2

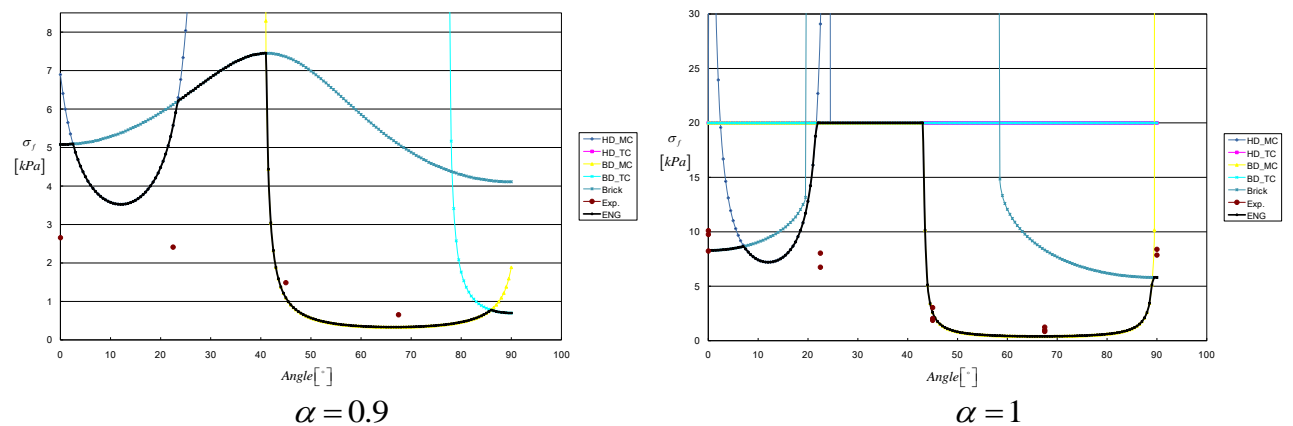


Fig. 2

It is seen from the results on the graphs that an engineering approach gives failure stresses close to the experimental values, in most situations. Experimental results in masonry have a large scatter one would not expect good matching with theoretical results. The Engineering Approach obtaining mechanical behaviour of masonry from that of constituents is promising and should be further investigated and used for verification purposes.

## 2. The Critical Plane Approach (CPA)

A rational approach to evaluate the behavior of unreinforced masonry under seismic loading should incorporate advanced nonlinear formulations that account for the diversity of mechanical characteristics. Mathematical procedures such as 'Critical Plane Approach' (CPA) [Ushaksarai & Pietruszczak (2002) Pietruszczak & Ushaksarai (2003), are show to be adequate for these evaluations.

The approach is primarily concerned with verification of a macroscopic failure criterion for structural masonry that is formulated within the framework of the critical plane approach (Pietruszczak, S. & Mroz, Z. 2001). The failure criterion is defined in a local sense, i.e. in terms of traction components acting on a physical plane, and its representation employs a set of distribution functions specifying the variation of strength parameters. The approach consists of identifying such an orientation of the critical or localization plane, for which the failure function reaches a maximum. An extensive numerical analysis should always be performed focussing on identification of material parameters/functions and verification of the critical plane approach. The latter is performed in two stages. The first one involves predictions of the conditions at failure in masonry panels subjected to biaxial compression-tension at different orientation of the bed joints relative to the loading direction. The second stage involves an initial boundary value problem, i.e. a dynamic analysis of multi-storey masonry building subjected to seismic excitation.

The explanation of the methodology is structured as follows. First, a brief review of the basic notions of the critical plane approach is provided. Subsequently, the results of numerical analyses are discussed. The question of identification of the material parameters is addressed first followed by the predictions of the conditions at failure in a series of biaxial tension-compression loading histories. Two sets of experimental data are used for the verification/validation purposes, i.e. Samarasinghe and Hendry [2] and Page [3]. In the follow up section, a homogenization procedure is discussed that is aimed at predicting the strength properties of masonry based on properties of constituent materials. Two different methodologies are used: finite element analysis of a Representative Elementary Volume (REV) subjected to periodic boundary conditions and a lower bound analysis. The latter gives estimates of macroscopic strength based on an optimization procedure that employs a simple statically and plastically admissible stress field. The homogenization procedure is then employed to identify the macroscopic properties of structural masonry used in physical model tests of IEEES, Skopje. Finally, the finite element simulations are carried out of a shaking table experiment that involves a four storey building (scale 1/3) subjected to cyclic loading (IEEES, Skopje).

## 2.1. Critical Plane Approach (CPA); formulation of the problem

The approach employs a spatial distribution of strength parameters and defines the conditions at failure in terms of traction components on the critical/localization plane. The orientation of this plane is determined by maximizing the failure function using a constrained optimization analysis.

Here, a linear Mohr-Coulomb failure function with a tension cut-off is adopted

$$F_1 = \tau + \sigma_n \tan(\varphi) - c = 0, \quad F_2 = \sigma_n - \sigma_0 = 0 \quad (1)$$

where  $\tau$  and  $\sigma_n$  are shear and normal components of the traction vector on the plane with unit normal  $n_i$ , respectively. Thus

$$\tau = \sigma_{ij} n_i s_j, \quad \sigma_n = \sigma_{ij} n_i n_j \quad (2)$$

where

$$s_i = t_i^s / \|t_i^s\|, \quad t_i^s = (\delta_{ij} - n_i n_j) \sigma_{jk} n_k \quad (3)$$

and  $t_i^s$  is the tangential component of the traction vector on this plane. In equation (1), the material parameters  $\sigma_0$ ,  $\varphi$ , and  $c$  are defined in terms of distribution functions

$$\begin{aligned} \sigma_0 &= \sigma_{01} (1 + \Omega_{ij}^{\sigma_0} n_i n_j) + \sigma_{02} (\Omega_{ij}^{\sigma_0} n_i n_j)^2 + \sigma_{03} (\Omega_{ij}^{\sigma_0} n_i n_j)^3 \\ \varphi &= \varphi_1 (1 + \Omega_{ij}^{\varphi} n_i n_j) + \varphi_2 (\Omega_{ij}^{\varphi} n_i n_j)^2 + \varphi_3 (\Omega_{ij}^{\varphi} n_i n_j)^3 \\ c &= c_1 (1 + \Omega_{ij}^c n_i n_j) + c_2 (\Omega_{ij}^c n_i n_j)^2 + c_3 (\Omega_{ij}^c n_i n_j)^3 \end{aligned} \quad (4)$$

in which  $\sigma_{01}, \sigma_{02}, \sigma_{03}, \varphi_1, \varphi_2, \varphi_3, c_1, c_2, c_3$  are the distribution coefficients and  $\Omega$  is a set of symmetric traceless tensors which describes the bias in the spatial variation of the strength parameters. The incorporation of higher order dyadic products of  $\Omega_{ij} n_i n_j$  allows for a more accurate representation of the material behaviour as pointed out in ref.[1]. The orientation of the localization plane can be determined by maximizing the failure functions  $F_1$ , and  $F_2$  with respect to  $n_i$  and  $s_i$ , subject to constraints

$$n_i n_i = 1; \quad s_i s_i = 1; \quad n_i s_i = 0 \quad (5)$$

Introducing Lagrange multipliers  $\lambda_1$ ,  $\lambda_2$ , and  $\lambda_3$ , the corresponding Lagrangian function for  $F_1$  becomes

$$G_1 = \sigma_{ij} n_i n_j + \tan[\varphi_1(1 + \Omega_{ij}^o n_i n_j) + \varphi_2(\Omega_{ij}^o n_i n_j)^2 + \varphi_3(\Omega_{ij}^o n_i n_j)^3] - c_1(1 + \Omega_{ij}^c n_i n_j) - c_2(\Omega_{ij}^c n_i n_j)^2 - c_3(\Omega_{ij}^c n_i n_j)^3 \quad (6)$$

The stationary conditions of  $G_1$  with respect to  $n_i$  and  $s_i$  are expressed as  $\partial G_1 / \partial n_i = 0$  and  $\partial G_1 / \partial s_i = 0$ , whereas the stationary conditions with respect to  $\lambda$ 's provide the constraints (5). The resulting set of algebraic equations can be solved for both the direction cosines  $n_i$  and  $s_i$ , as well as  $\lambda$ 's. Given  $n_i$  and  $s_i$ , the first criterion in eq. (1) can then be verified to determine whether the conditions at failure have been reached. The same procedure can be employed for the second failure function in equation (1). In this case, the Lagrangian function becomes

$$G_2 = \sigma_{ij} n_i n_j - \sigma_{01}(1 + \Omega_{ij}^{\sigma_0} n_i n_j) - \sigma_{02}(\Omega_{ij}^{\sigma_0} n_i n_j)^2 - \sigma_{03}(\Omega_{ij}^{\sigma_0} n_i n_j)^3 \quad (7)$$

After solving for  $n_i$ ,  $s_i$ , and  $\lambda$ 's, the second criterion in eq. (1) can be checked to determine whether the conditions at failure have been reached. The governing failure function is that for which  $\max\{F_1, F_2\} = 0$ . More details regarding the numerical procedure can be found in (Ushaksaraei R. & Pietruszczak S. 2002).

## 2.2. Identification and verification of CPA; tests on masonry panels

In what follows, the results of numerical simulations for the validation of the critical plane approach are presented. First, the question of identification of material parameters involved in the distribution functions is addressed. Subsequently, the formulation is applied to examine the conditions at failure in a brickwork panel. In particular, a series of biaxial tension-compression loading histories is simulated for different orientation of bed joint relative to the loading direction. Two different sets of experimental data reported in literature have been used, viz. Samarasinghe and Hendry 1982 and Page 1983. In what follows, the performance of CPA is examined in the context of both these series of tests.

Fig 1 defines the geometry of the problem and the loading conditions. Figs. 3-8 show comparisons between the results of the critical plane approach and the experimental data, for the tests used in the identification process. The figures show the variation of strength with the sample orientation. The simulations for validation/verification of CPA are provided in the set of Fig. 3-5 (comparison with the experimental results of Samarasinghe and Hendry 1982. Fig. 4 show the results for the trajectories involving  $\alpha=0.4$ , 0.75 and 0.8, respectively. Figure 5 show the strength envelopes in biaxial tension-compression for a set of discrete orientations of bed joints, viz.  $0^\circ$ ,  $45^\circ$ , and  $90^\circ$ , respectively.

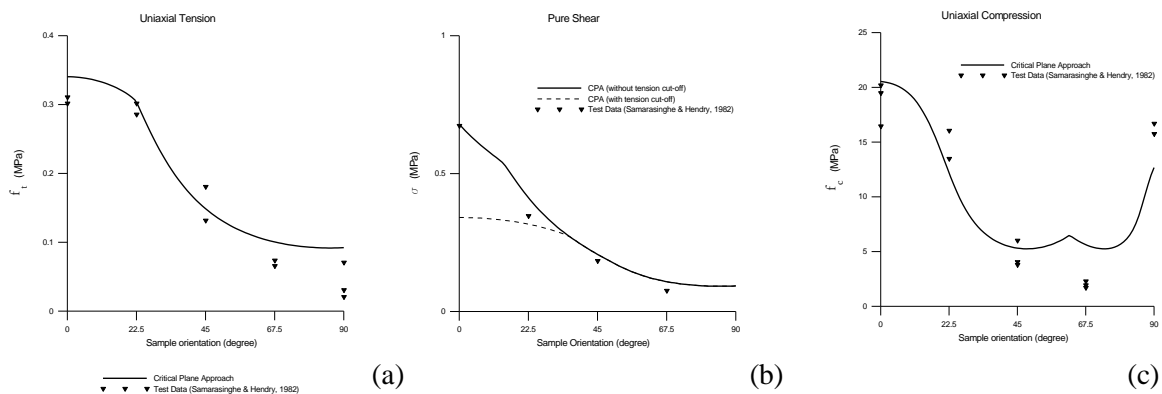


Fig. 3 Variation of (a) uniaxial tensile strength, (b) pure shear and (c) uniaxial compressive strength, with

sample orientation (Samarasinghe and Hendry 1982)

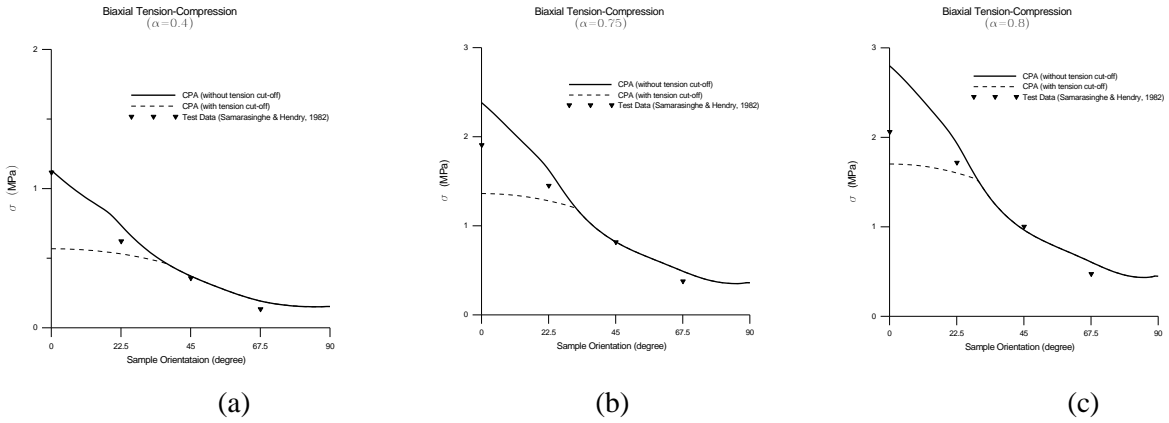


Fig. 4 Variation of strength with sample orientation for: (a)  $\alpha=0.4$ , (b)  $\alpha=0.75$ , and (c)  $\alpha=0.8$  (Samarasinghe and Hendry 1982)

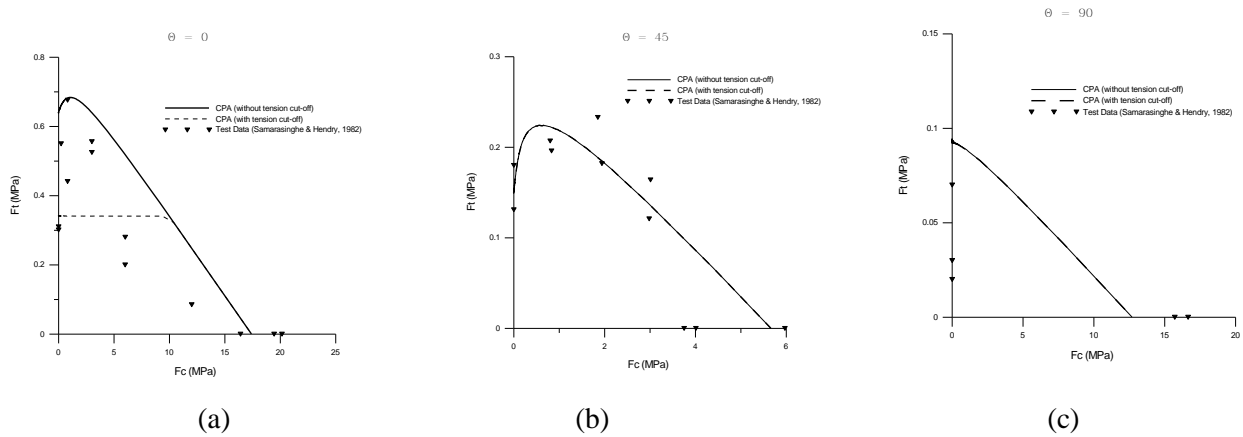


Fig. 5 Failure envelope for in-plane biaxial tension-compression test for: (a)  $\theta=0^\circ$ , (b)  $\theta=45^\circ$  and (c)  $\theta=90^\circ$  (Samarasinghe and Hendry 1982)

The simulations for validation/verification of CPA are provided in the set of Fig. 6-8 (comparison with the experimental results of Page 1983). Fig. 6 show the results for the trajectories involving  $\alpha=0.4, 0.75$  and  $0.8$ , respectively. Figure 7 show the strength envelopes in biaxial tension-compression for a set of discrete orientations of bed joints, viz.  $0^\circ, 45^\circ$ , and  $90^\circ$ , respectively.

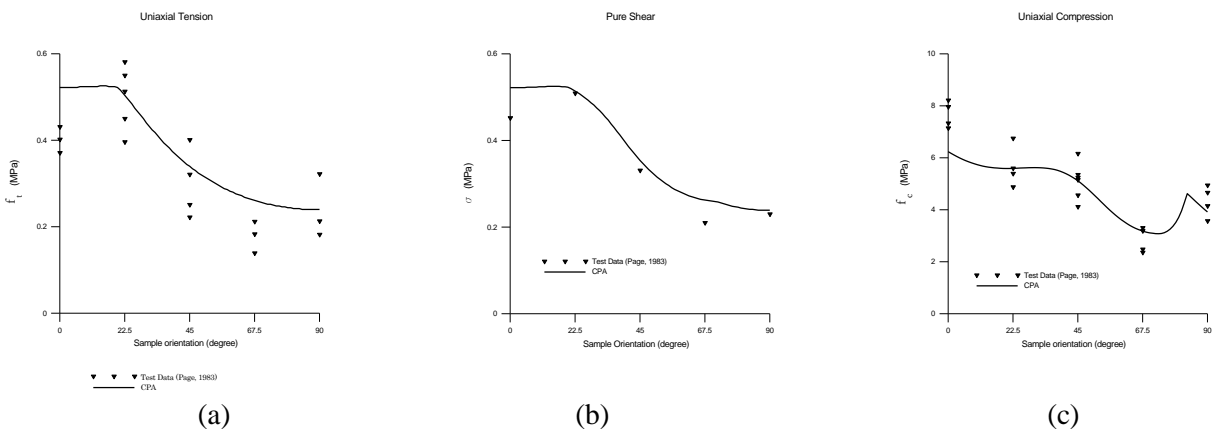
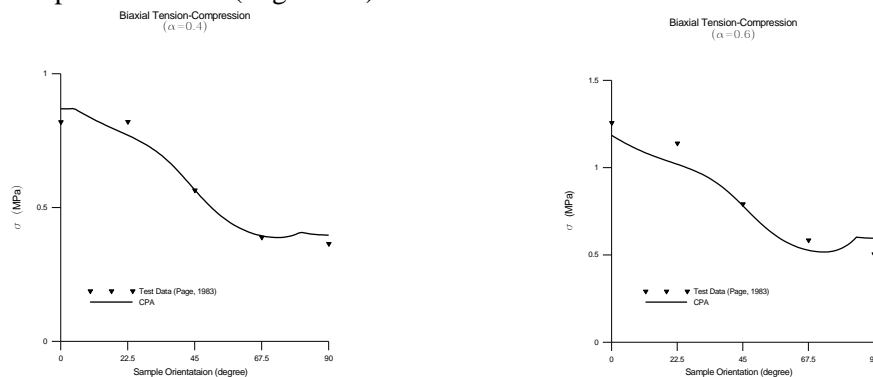


Fig. 6 Variation of (a) uniaxial tensile strength, (b) pure shear and (c) uniaxial compressive strength, with sample orientation (Page 1983)



(a) (b)  
 Fig. 7 Variation of strength with sample orientation for: (a)  $\alpha = 0.4$ , and (b)  $\alpha = 0.6$ , (Page 1983)

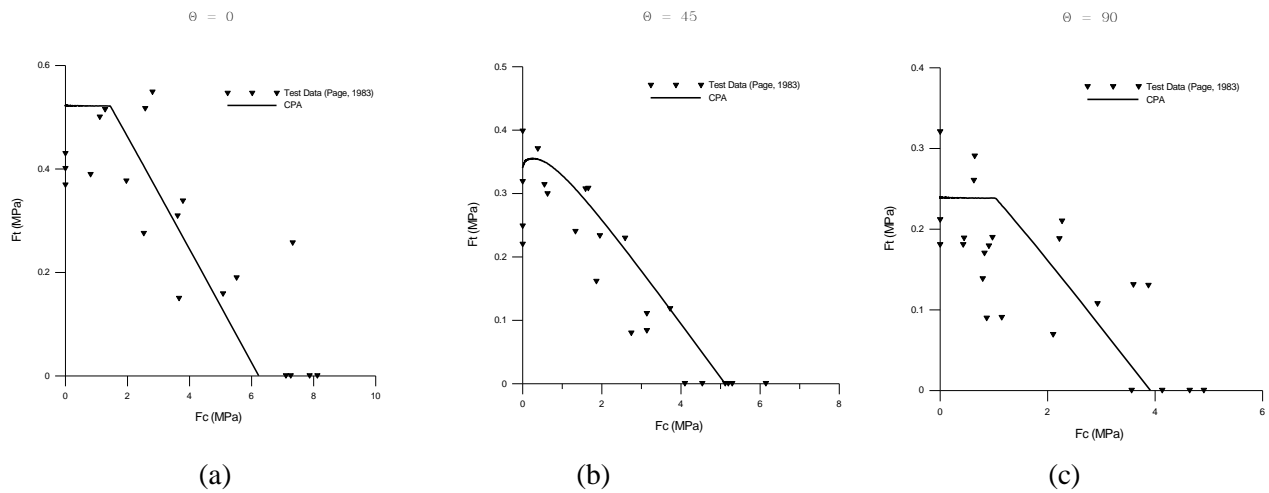


Fig. 8 Failure envelope for in-plane biaxial tension-compression test for: (a)  $\theta = 0^\circ$ , (b)  $\theta = 45^\circ$  and (c)  $\theta = 90^\circ$  (Page 1983)

### 3. Homogenization procedures for predicting strength properties of masonry

Masonry may be considered as a composite material comprising brick units and mortar joints in a periodic arrangement. Thus, the average mechanical behaviour of structural masonry can be estimated from the properties of its constituents using a homogenization procedure. This approach is particularly useful in case when the experimental results on masonry panels are not available and the only information given is that on properties of mortar and the masonry units. In general, different homogenization techniques can be employed for predicting the strength properties of masonry. Here, two different approaches are implemented and explained. The first one is a numerical homogenization based on finite element analysis. It employs a Representative Elementary Volume (REV) of masonry subjected to periodic boundary conditions. The analysis was conducted for an elastic-perfectly plastic Mohr-Coulomb material with a tension cut-off and it incorporated an associated flow rule. The second approach is an assessment based on lower bound analysis that invokes constructing a statically and plastically admissible stress field and optimizing the parameters to obtain the maximum value of the ultimate load.

In this section, the predictive abilities of both approaches are examined by comparing the performance with the experimental data of Samarasinghe and Hendry [2]. Subsequently, this proposed methodology is applied to identify the critical plane parameters representative of structural masonry used in physical model tests of Institute of Earthquake Engineering & Engineering Seismology (IEEES) at Skopje. Finally, the finite element simulations of a shaking table experiment are carried out. The latter involve a four storey building (scale 1/3) subjected to cyclic loading (IEEES, Skopje). The assessment of cracked zones is based on dynamic analysis incorporating elastic orthotropic properties of masonry and subsequent evaluation of plastic admissibility of the resultant stress field.

#### 3.1. Finite element analysis for periodic REV

The first and perhaps the most accurate approach for predicting the average macroscopic properties of masonry is a numerical homogenization. Because of the periodic nature of masonry, it is not necessary to consider the whole panel. Here, a typical unit cell (REV) including brick and mortar joints has been discretized with properly modified boundary conditions that reflect the periodic nature of the structural arrangement. The discretization incorporated a number of 8-noded solid elements, see Fig. 9. For the nonlinear analysis, the force-controlled loading strategy has been used. A linear Mohr-Coulomb failure function with a tension cut-off was employed for the constituents, which were assumed to be elastic-perfectly plastic (no hardening/softening effect). The material parameters used in the numerical study were selected based on the experimental data provided in ref. Samarasinghe, W., Hendry, A. W. (1982).

### 3.2. A lower bound assessment

The second approach involves a limit state analysis based on the framework of homogenization. The procedure is based on a lower bound analysis whereby a plastically admissible stress fields are constructed in the constituents involved, subject to periodic boundary conditions and static equilibrium requirements. The critical load is obtained by solving a constrained optimization problem. The mathematical details of this approach are provided in ref.: Pietruszczak, S., Shieh-Beygi, B., and Kawa, M. (2006).

The results, corresponding to the same loading configuration as before (i.e. uniaxial tension and pure shear), are shown in Fig. 10. The lower bound approach leads to a conservative estimate of the strength. This is evident from both figures as the predictions based on the lower bound analysis fall below those obtained from the finite element analysis of REV.

In general, the predictions based on both homogenization approaches are quite reasonable, thereby providing some degree of confidence in the proposed methodology. Thus, in situations when the experimental information is restricted to properties of constituents only (which is the case for majority of the masonry walls of buildings), the average properties of masonry may be estimated by invoking one of the approaches identified here.

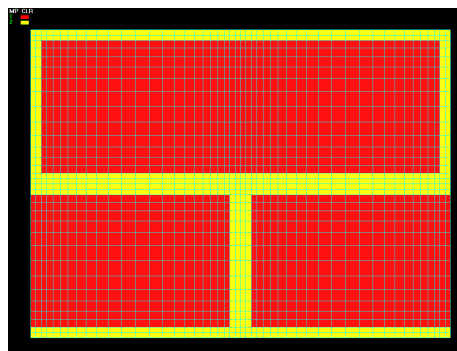


Fig.9 Geometry of REV

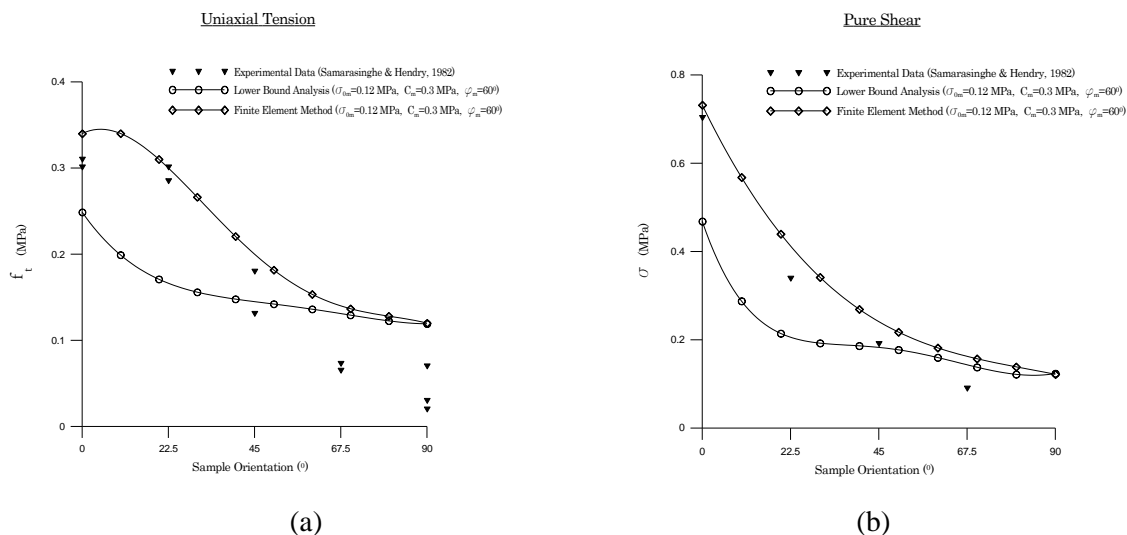


Fig. 10 Variation of strength with sample orientation for (a) uniaxial tensile strength and (b) for pure shear

### 4. Identification and verification of CPA; IEEEES, Skopje test

The validation of any new approach is completed by comparing the results obtained by simulation of a large boundary value problem and those obtained from the shaking platform test of the same problem. Here, the results of finite element simulations of a shaking table experiment, as conducted by IEEEES Skopje, are presented. The experiment involved a four storey masonry building subjected to cyclic loading simulating an earthquake excitation. The numerical study involves a dynamic elastic analysis

incorporating orthotropic properties, which is supplemented by an assessment of plastic admissibility of the stress field based on the critical plane approach.

For the problem analysed here, no experimental results on properties of structural masonry are available. The only information provided is that on basic strength properties of constituents. Thus, the methodology employed here involves first the application of the homogenization theory incorporating lower bound analysis to assess the macroscopic strength properties in uniaxial tension, pure shear and biaxial compression-tension ( $\alpha=0.4$ ). Given this assessment the material parameters for the critical plane approach are then identified. Subsequently, the finite element simulations are carried out at the structural level and the results are compared with experimental data reported in the ref. Report IZIIS No. 9/66 (1989).

#### 4.1. Specification of material parameters

The limit state analysis based on homogenization approach has been used to predict the strength properties of masonry. The properties of constituents have been estimated based on the data reported in ref. Report IZIIS No. 9/66 (1989). The values of the basic parameters were chosen are presented in Table 2.

Three distinct loading configurations have been considered for the specification of parameters for the critical plane approach; viz. uniaxial tension, pure shear, and biaxial tension-compression for  $\alpha = 0.4$  (see Fig. 1). The plots showing the variation of strength of the masonry with sample orientation, for all loading histories considered, are shown in figures 11-12. The results of these simulations have been used for identification of the parameters involved in the macroscopic failure function.

Table 2

Material	Parameter	Value
Brick	$\varphi_b$	$55^\circ$
	$c_b$	2.38 MPa
	$\sigma_{0b}$	1.5 MPa
Mortar	$\varphi_m$	$50^\circ$
	$c_m$	0.35 MPa
	$\sigma_{0m}$	0.15 MPa

The first set of data, shown in Fig. 11, was employed for specification of the parameters embedded in the distribution of  $\sigma_0$ , eq.(4). The details on the identification procedure are provided in Appendix A. The results depicted in Fig. 12 were then used for specification of constants appearing in the distribution of  $\varphi$  and  $c$  (see Appendix B). The resulting values of the material parameters are as follows:

$$\begin{aligned} \Omega_1^{\sigma_0} &= 0.350234; & \sigma_{01} &= 0.208776; & \sigma_{02} &= 0.538448; & \sigma_{03} &= 0.514172 \\ \Omega_1^\varphi &= 0.587833; & \varphi_1 &= 54.7978; & \varphi_2 &= -69.7379; & \varphi_3 &= -115.071 \\ \Omega_1^c &= 1.1; & c_1 &= 0.669701; & c_2 &= 2.2815; & c_3 &= 0.814019 \end{aligned} \quad (11)$$

Given the above set of parameters, the back-analysis has been carried out simulating the considered loading histories. In Figs. 11-12 the results for CPA, shown by a solid line, are compared with lower bound estimates from the homogenization approach. Fig. 12 shows the prediction for the biaxial tension-compression test at  $\alpha = 0.6$  (i.e the Uniaxial Tension magnitude of compressive stress is 4 Pure Shear times that of tensile stress, Fig.1).

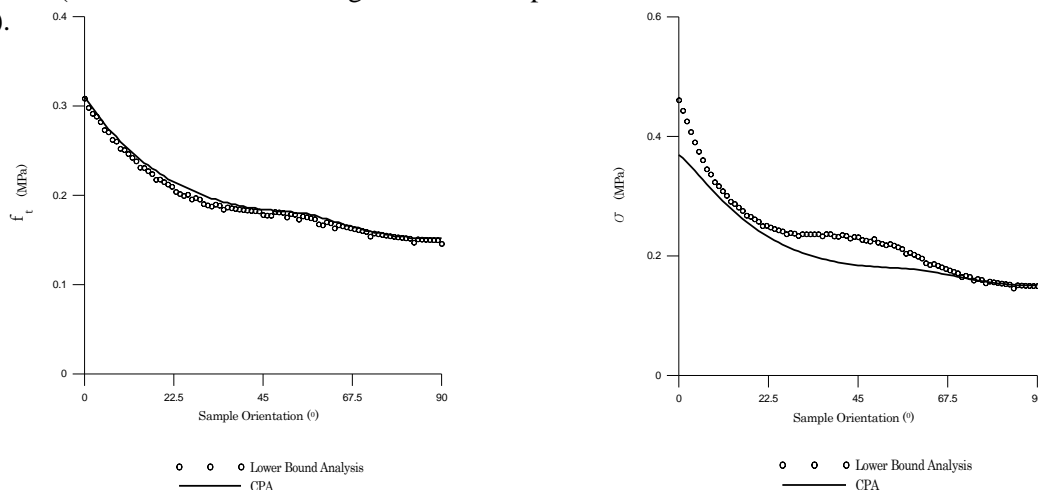


Fig. 11 Variation of uniaxial tensile strength and for pure shear with sample orientation

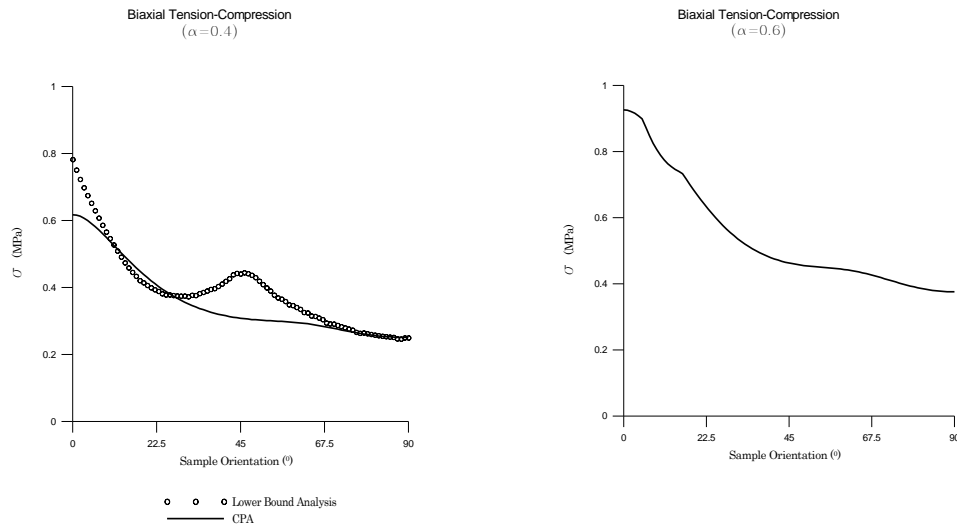


Fig. 12 Variation of strength with sample orientation for  $\alpha = 0.4$  and  $\alpha = 0.6$

#### 4.2 Finite element simulation of a test on a masonry building (scale 1/3) subjected to cyclic loading

The main results of finite element simulations of the reduced scale model test of IEEEES Skopje, are briefly reviewed. The physical experiment involved a shaking table test conducted on a four storey building (scale 1/3) subjected to cyclic loading that simulated an earthquake excitation. The results of this experiment are described in details in ref. Report IZIIS No. 9/66 (1989). The dynamic finite element simulations were performed in elastic range, assuming orthotropic material properties, and the plastic admissibility of the resulting stress fields was assessed based on the macroscopic failure criterion (1) incorporating the constants evaluated in eq.(11). The predicted failure zones have been compared with those recorded experimentally.

The finite element discretization of the building and its masonry walls R-1, R-2, and R-3 is shown in Fig.14. The total of 8,786 8-noded solid elements (masonry walls as well as concrete foundation and floors) was used. Figure 13 shows the ground motion history for which the analysis was conducted. The maximum horizontal acceleration was fixed at 0.5091g. The analysis was conducted using the following set of orthotropic elastic properties of masonry:

$$\begin{aligned}
 E_x &= 1.5 \times 10^9 \text{ MPA}; & E_y &= 1.0 \times 10^9 \text{ MPA}; & E_z &= 1.8 \times 10^9 \text{ MPA}; \\
 G_{xy} &= 6.0 \times 10^8 \text{ MPA}; & G_{yz} &= 3.6 \times 10^8 \text{ MPA}; & G_{xz} &= 3.6 \times 10^8 \text{ MPA}; \\
 \nu_{xy} &= 0.24; & \nu_{yz} &= 0.24; & \nu_{xz} &= 0.14;
 \end{aligned}
 \tag{12}$$

The above parameters were estimated based on a homogenization approach outlined in ref.: Pietruszczak S., Niu X. (1992), and the values are referred to the geometry of wall R-2, as depicted in Fig.14.

Figure 15 shows the maps of the value of the failure function, eq.(1), for the masonry walls. The results for the crack pattern obtained from the shaking table test are also depicted in this figure. It is evident that the extent of the damage as predicted by numerically is fairly consistent with the experimental observations.

Finally, a comparison between the measured and predicted values of accelerations, at different elevations within the building, has been performed. In the shaking table experiment, the measurements were taken at the base of the model and at all consecutive floors. Figure 13 shows the input acceleration applied at the base. Figure 16 present the acceleration histories at the base and at the 4th floor recorded in experiment together with those predicted by the finite element analysis. In general, it is evident that the agreement between the two sets of accelerations, at all different levels of the building, is quite reasonable.

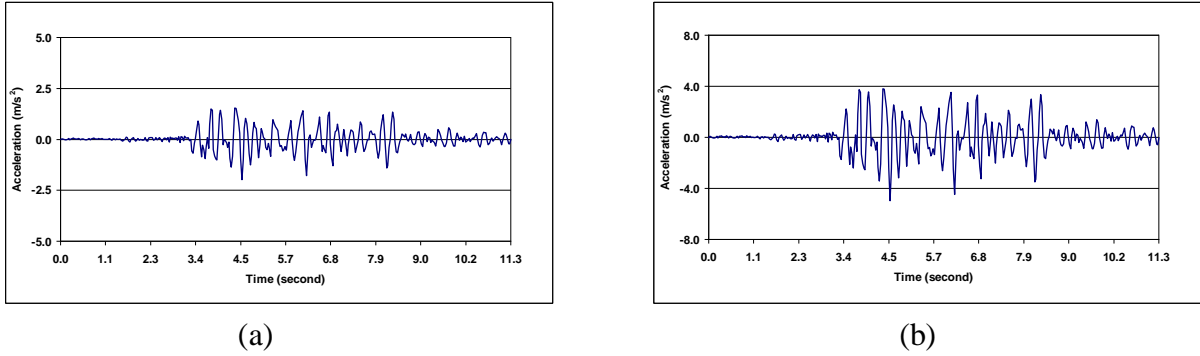


Fig. 13 Input acceleration curve (max. acceleration: (a) 20.37%g and (b) 50.91%g at 4.56 seconds)

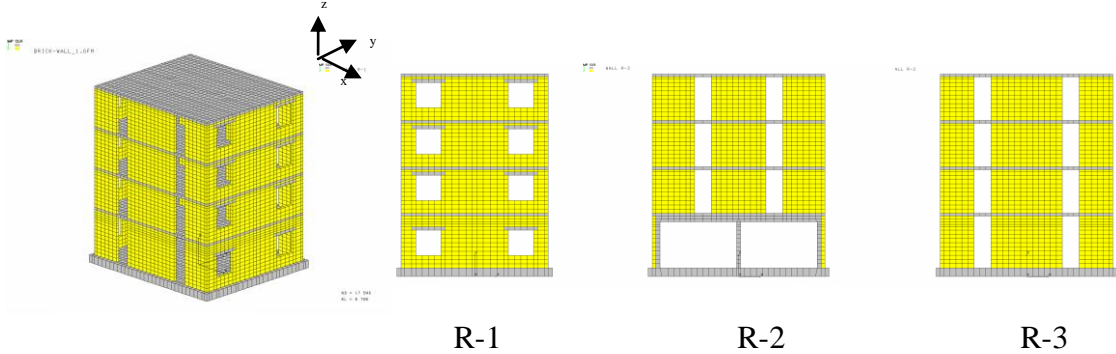


Fig. 14 Concrete-masonry-blocks model Finite element discretization of the building and the walls R-1, R-2, and R-3

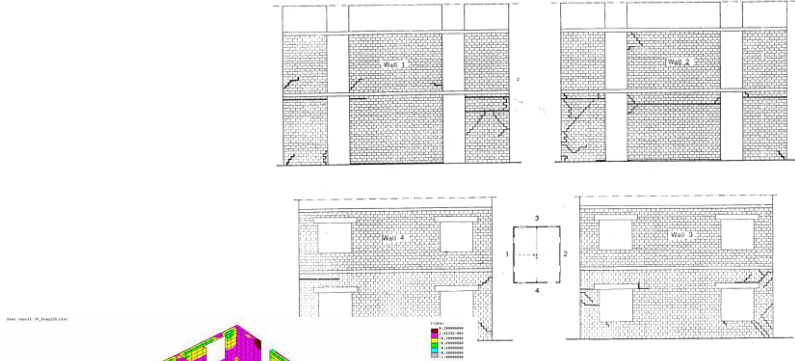


Fig 15(a) Crack patterns of the tested walls

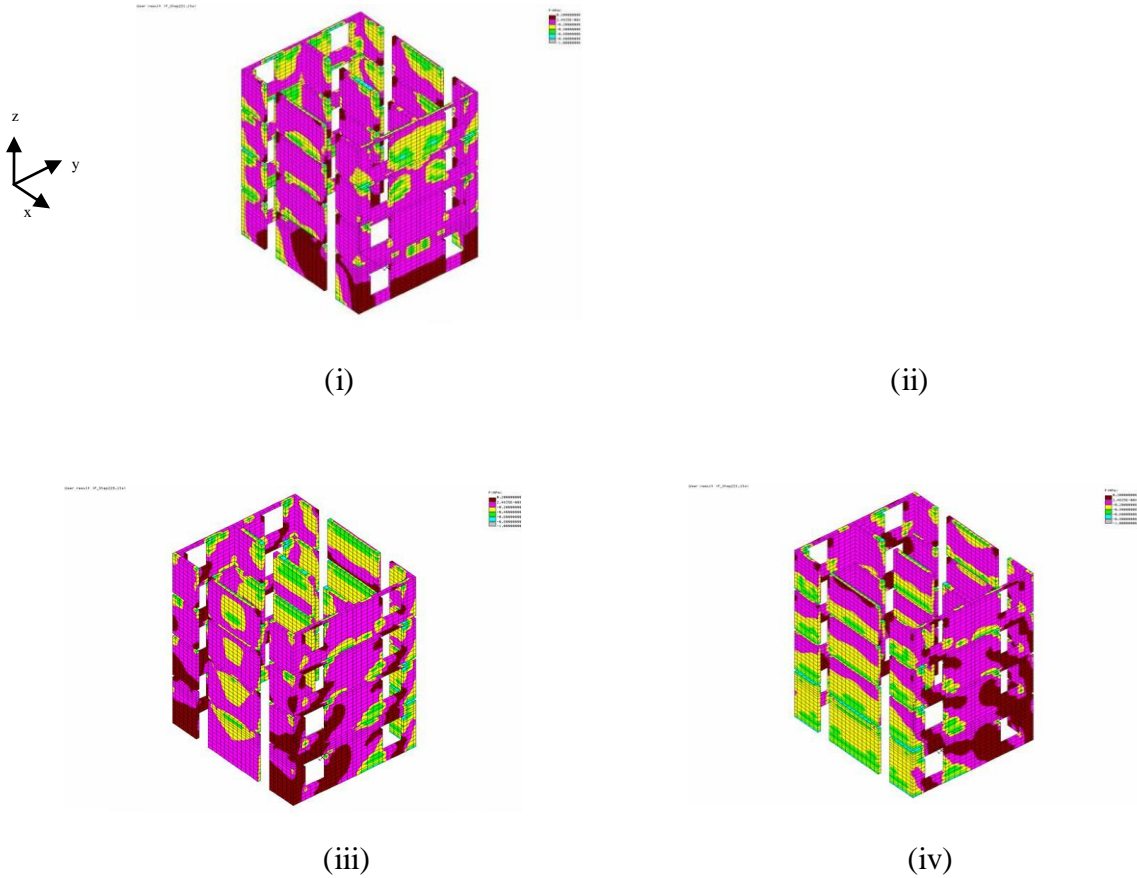


Fig. 15(b) Maps of failure function for the analysed structure. Excitation along the direction of x (top figures) and y (bottom figures); distributions correspond to maximum displacement in the direction of (i) +x, (ii) -x, (iii) +y, (iv) -y

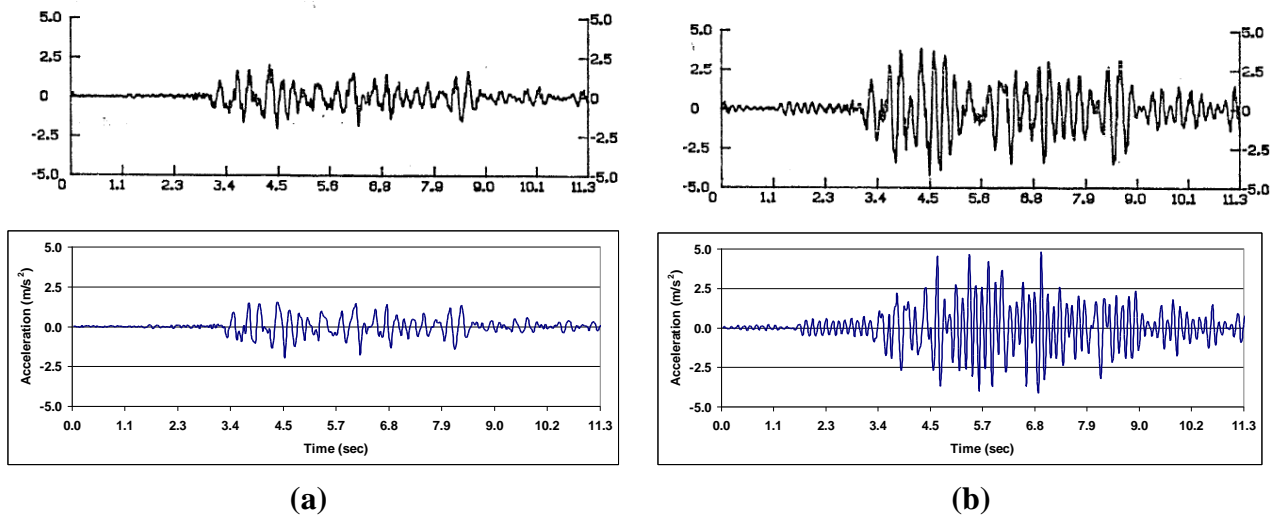


Fig. 16 Acceleration histories at the base (a) and at the 4th floor (b); measured (top figure) and predicted (bottom figure)

The primary objective of the work reported in section 4 is the validation/verification of the performance of the critical plane approach. This was conducted in two separate stages. First, the results on masonry panels tested by Samarasinghe and Hendry and Page were simulated. The methodology employed here involves identification of material parameters/functions of CPA based on a series of three independent tests, i.e. uniaxial tension, pure shear and uniaxial compression. Given the values of material parameters, an extensive verification was performed aimed at predicting the failure envelopes in biaxial compression-tension at different orientations of the sample relative to the loading direction. The results of simulations are, in general, in a fairly good agreement with the experimental data.

The second stage of the verification process is concerned with a simulation of a shaking table experiment that involved an out-of-plane action. The methodology employed here is similar to that advocated

for examining the response of masonry walls of numerous important structures such as powerhouses, hospitals, schools, historical buildings, etc. Namely, the first step involves assessment of macroscopic properties of structural masonry based on a homogenization procedure. Here, two independent approaches were investigated, viz. (i) numerical homogenization employing a Representative Elementary Volume (REV) of masonry subjected to periodic boundary conditions and (ii) a lower bound estimate based on limit analysis. Given the macroscopic strength properties, the material parameters for CPA can then be defined following the identification procedure outlined in this report. The predictive abilities of the proposed methodology were examined by comparing the performance with the experimental data of Samarasinghe and Hendry. Subsequently, the lower bound approach was applied to identify strength properties of structural masonry used in physical model tests of IEEEES, Skopje. Finally, the finite element simulations of a shaking table experiment were carried out and the key results were compared with the experimental record.

The presented verification procedure combined with elaborate in-situ and laboratory testing of masonry constituents defines the CPA as a powerful and appropriate analytical tool that provides possibility of adequate structural evaluation and reinforcement (if required) of structures exposed to static and seismic loadings.

## 5. Numerical analysis of a brick masonry structure

An example of the application of the CPA on a two story unreinforced masonry building is presented next. The building comprises of a basement, a ground floor and one floor above ground. It is composed of reinforced concrete frames and slabs. Unreinforced two layers non-bearing masonry walls serve as enclosures. The outside layer is continuously constructed of bricks for the entire height of the building while the internal layer build of bricks (bottom half of the storey height) and concrete blocks (upper half of the storey height) is incorporated as infield panels between the columns. The laterally unsupported height of the walls is the entire storey height of 6.5 m. The outside view, the geometry of the building and the finite element (FE) model employed in the non-linear dynamic analysis using the above described procedure are presented in Fig. 17. The results of the elaborated analysis are shown in Fig. 17 as well.

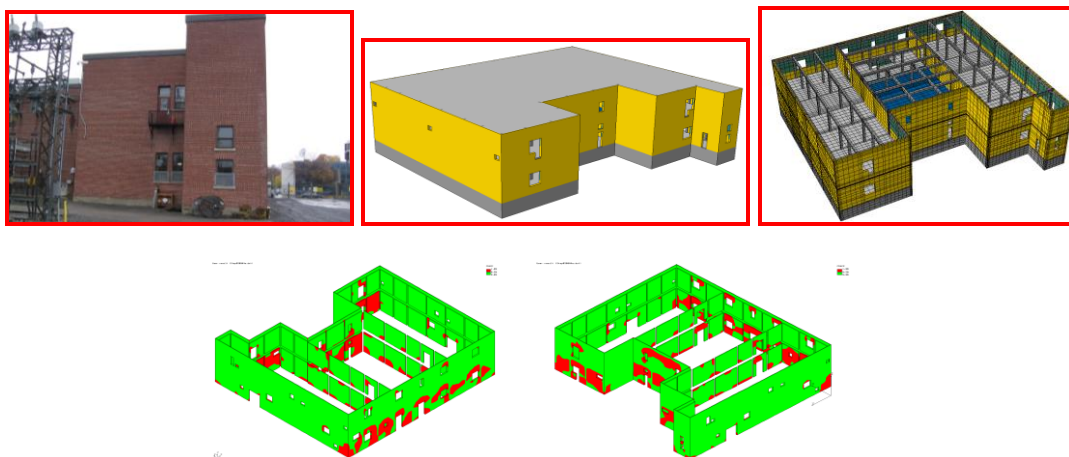


Figure 17. The geometry of the building, and the results of the elaborate FE dynamic analysis. The red areas indicate distribution of cracks in the masonry walls.

In order to specify the material properties, a series of in-situ experimental shear tests was performed on the brick walls. The procedure involved extracting two alternate bricks from a single row of the brickwork and subjecting the remaining brick to a horizontal load. In this way, the in-situ shear strength of the mortar can be assessed which, in turn, can give an indication of its tensile strength. In addition, the bricks extracted from the wall were tested for compressive and tensile strengths. Based on the experimental results, the basic material properties were established for constituents. Using those values, the average macroscopic properties of masonry were assessed, as discussed in Section 4. An important step of the validation process was the evaluation of the dynamic response of the analysed structure. The in-situ measurements of ambient vibrations

were performed and the obtained natural frequencies and mode shapes were compared with those obtained from the numerical analysis.

The results of the numerical analysis showed that the story drifts as well as the max structural deformation are greater than the tolerances required by the NBC of Canada for structure used as a public safety building. Hence, strengthening of the building was required. Steel bracing combined with “System DC90” dampers are employed. The adequate choice of dampers depends on the in-plane rigidity of the masonry walls of the building and their capacity to participate with the dampers in the seismic energy dissipation. A simplified numerical analysis is proposed in order to reduce the time requirements of the elaborated FE non-linear dynamic analysis. The dynamic characteristics of typical masonry walls (panels) are evaluated following the macro-scale approach as described in Section 3 using the FE program COSMOS/M and then replaced with equivalent “Link” elements of SAP2000 software. For the analyzed building six typical panels were defined as shown on Fig. 18a. For each panel

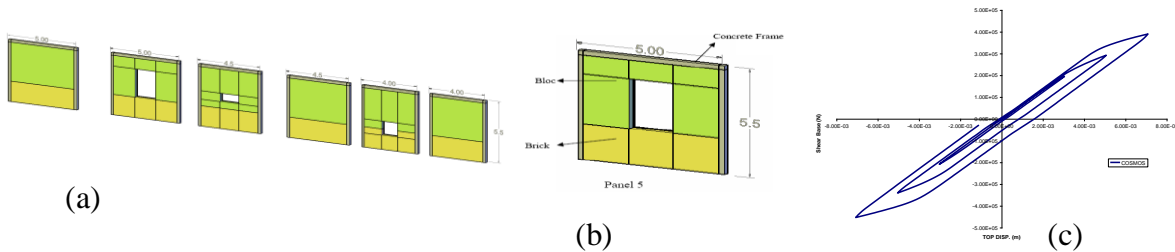


Figure 18. Typical masonry panels (a); panel #5 (b) and its shear force-deformation hysteresis (c)

(such as panel #5 shown on Fig. 18b) the force-deformation hysteresis diagram Fig. 18c was defined by elaborate FE panel analysis using COSMOS/M software. The equivalent “Link” element having the force-deformation hysteresis diagram closely matching the one obtained for the masonry panel is used in the global building model replacing the masonry panel Fig. 19.

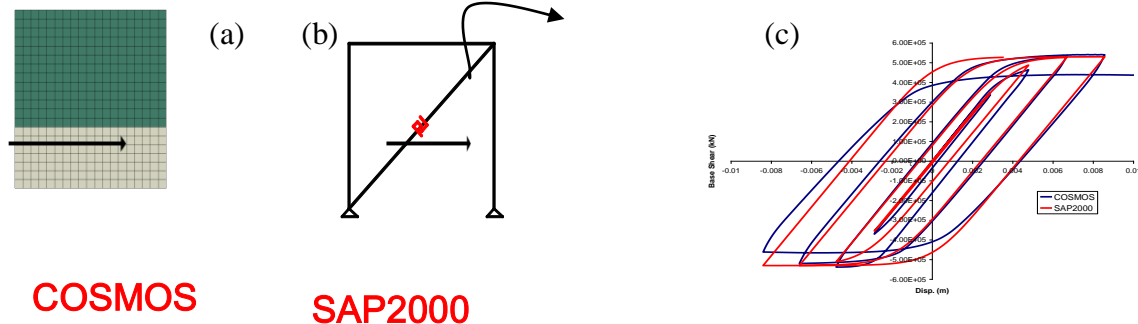


Figure 19. Typical masonry panel (a); replaced by “Link” element (b); having equivalent hysteresis (c)

The numerical model including the “Link” elements is shown on Fig. 20a. Six (6) sets of bracings Figs. 20b and 20c incorporating twelve (12) dampers were added. The required mechanical characteristics of the dampers and their optimal location in the building were obtained numerically by performing several analyses. The procedure of finding an adequate number and suitable type of dampers able to dissipate energy together with the masonry walls is the most important part of the analysis.

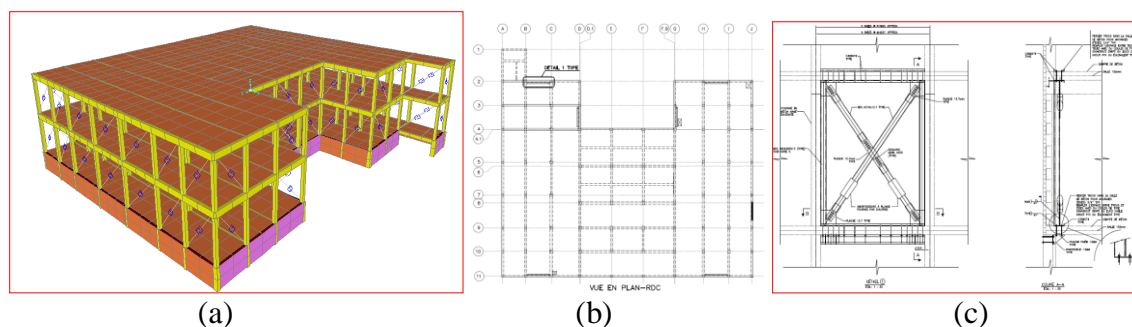
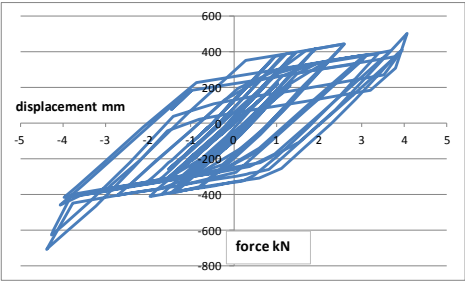
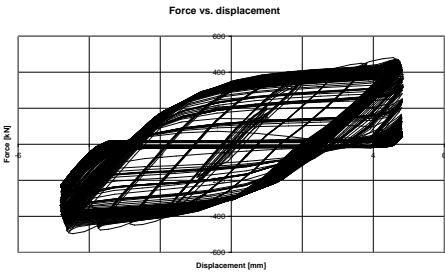


Figure 20. Numerical model including the “Link” elements in SAP2000 (a); location of the bracings with dampers on the ground floor of the building (b); and unit of bracing with dampers (c)

The selection of dampers and the bracing struts, with their stiffness characteristics, is function of the rigidities and the performance of the masonry walls. Hence, they are different for each building and are therefore usually custom made. Fig. 21a represents an optimized damper and for the analyzed building structurally adequate, numerically obtained, damper characteristics. Based on the calculated hysteresis diagram the supplier (System DC90) has fabricated and tested the dampers. Fig. 21b presents the results of their test.



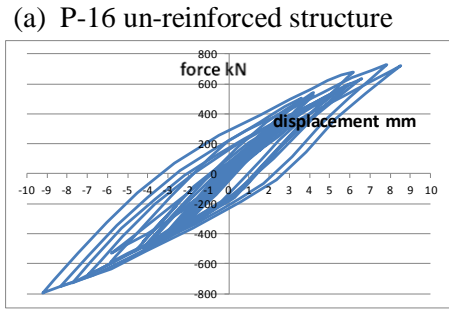
(a) D-98 Damper 1.5 to 4.0 mm; 320 to 420 kN



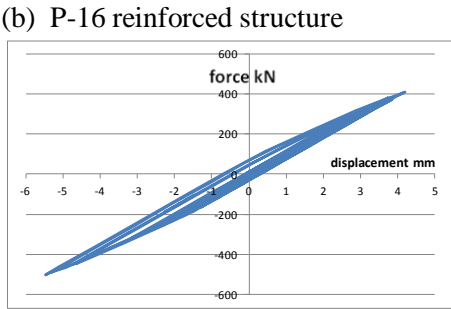
(b) Damper 1.5 to 4.5 mm; 450 kN (test)

Figure 21. Hysteresis obtained from the analysis (a); Results from the test (b)

The strengthening of the building with steel bracings, anchored to the concrete frame, combined with “System DC90” dampers for energy dissipation was sufficient to fulfill the requirements of the NBC of Canada for drift limitation and maximum total deformation of the unreinforced masonry public safety building. The hysteresis diagrams of a typical masonry panel before Fig. 22a and after the added reinforcement Fig. 22b, indicates reduction of the deformations to a level acceptable by the NBC. It can be seen that the dampers are dissipating large portion of the seismic energy and in the same time preventing the masonry of excessive deformation and cracking.



(a) P-16 un-reinforced structure



(b) P-16 reinforced structure

Figure 22. Hysteresis for a typical masonry panel obtained from the analysis: (a) before and (b) after the structural reinforcement with bracings and dampers

6. Final remarks

The work reported here presents a simple and effective strategy for analysing and reinforcing the non-bearing masonry walls in case of a seismic event. This study clearly demonstrates that, given the complexity of the structure, a conventional approach, based on simplistic standards/guidelines adopted by consulting engineering offices, would not be adequate here. In this case, an appropriate finite element analysis is required, examining the history of loading, to asses the efficiency of the proposed refurbishing strategy.

The macroscopic failure criterion applied to evaluate the areas of potential damage (rather than an intuitive judgement based on the values of individual stress components) represents an additional step in the proper assessment of the destructive nature of the seismic forces. The authors trust that the obtained results will be of valuable insight in assessing the methodology of strengthening the walls in the upcoming refurbishing works.

## References

- Gocevski V., 2007. Centrale de Beauharnois – Analyse et confortement sismique de l'enveloppe de la centrale. *Rapport D'avant-projet, Hydro-Québec Unité Structure, RPOOW 12242 001 – STR.*
- Zienkiewicz O. C. & Pande G. N. 1977. 'Time dependent multi-laminate model of rocks - a numerical study of deformation and failure of rock masses', *Intl. Jl. Num. & Analytical Meth. in Geomechanics*, September, 1977, Vol.4, No.3 pp 219- 247.
- Pande G.N., Beer G. & Williams J.R. 1990. *Numerical Methods In Rock Mechanics*, John Wiley & Sons, 1990
- Samarsinghe, W. & Hendry, A. 1980. 'The strength of brickwork under biaxial tension- compression, Proc. 7<sup>th</sup> Int. Symp. Load Bearing rickwork, London, 1980.
- Samarasinghe, W., Hendry, A. W. (1982). "Strength of brickwork under biaxial tensile and compressive stress.". *Proc. Br. Ceram. Soc.*, 30, 129-139.
- Page, A. W. (1983). "The strength of brick masonry under biaxial tension-compression.". *Int. J. Masonry Constr.*, 3(1), 26-31.
- Pietruszczak, S., Mroz, Z. 2001. "On failure criteria for anisotropic cohesive-frictional materials.". *Int. J. Numer. Analyt. Meth. Geomech.*, 25, 509-524.
- Ushaksaraei R. & Pietruszczak S. 2002. Failure criterion for structural masonry based on critical plane approach. *J. Eng. Mech. ASCE* 128(7): 769-778
- Pietruszczak S. & Ushaksaraei R. 2003. Description of inelastic behaviour of structural masonry. *Int. J. Solids & Structures* 40(15): 4003-4020.
- Pietruszczak, S., Shieh-Beygi, B., and Kawa, M. (2006). "Limit states for brick masonry based on a homogenization approach". *Intern. Journ. Solids & Struct.*
- Report IZIIS No. 9/66 (1989), "Basic and applied research study for seismic modeling of mixed reinforced concrete-masonry buildings", prepared by Bologna University & the Institute of Earthquake Engineering and Engineering Seismology (IEEES) of Skopje .
- Pietruszczak S., Niu X. (1992). "A mathematical description of macroscopic behaviour of brick masonry". *Intern. Journ. Solids & Struct.*, vol. 29, 531-546.

## Appendix A

In this section, the procedure for identification of the parameters embedded in the distribution function  $\sigma_0$ , eq.(4), is briefly outlined. In this case, the experimental results for uniaxial tension are employed (after ref.[2]). For each sample orientation, the variation of critical normal stress  $\sigma_n$  is established first, using the ultimate strength of the panel (see Fig. A1).

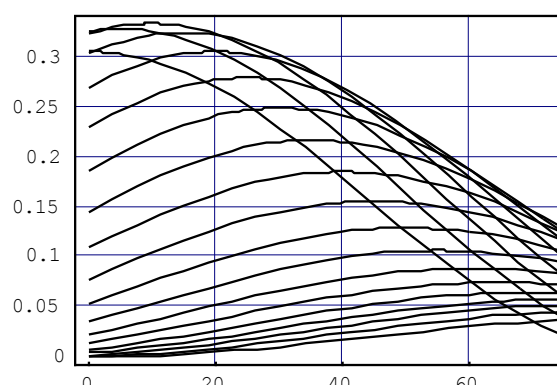


Fig. A1 Variation of  $\sigma_n$  for different tests

Subsequently, the envelope of the maximum values of normal stress,  $\sigma_{(envelope)}$ , is determined, as depicted in figure A2.

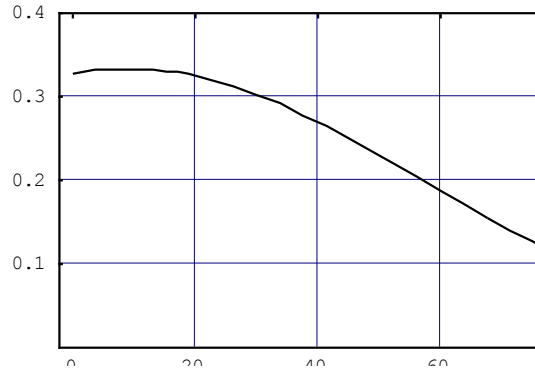


Fig. A2 The envelope of the maximum values of  $\sigma_n$ 's

A constrained optimization analysis is performed next to identify the constants involved, using a least-square best fit. For the tests of Samarasinghe and Hendry [2] the following values of material parameters are obtained:

$$\Omega_1^{\sigma_0} = 0.197204; \quad \sigma_{01} = 0.292111; \quad \sigma_{02} = -0.328489; \quad \sigma_{03} = 0.442279 \quad (A1)$$

The corresponding distribution of tensile strength  $\sigma_0$  is shown in figure A3.

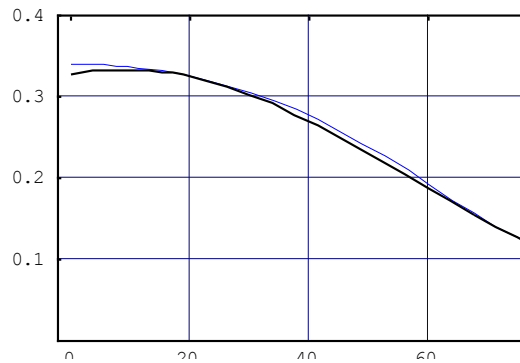


Fig. A3 The distributions of  $\sigma_{(envelope)}$  and  $\sigma_0$

## Appendix B

In this appendix, the procedure for identification of constants embedded in the spatial distribution of  $\varphi$  and  $c$ , eq.(4), is briefly discussed using, once again, the results of Samarasinghe and Hendry [2]. In this case, two sets of the experimental data are used, viz. the variation of strength with sample orientation in pure shear and uniaxial compression. In general, a unique value of  $\varphi$  and  $c$  should be associated with each plane for these two different sets of data. This provides a set of equations for identification of the “ideal” distributions for  $\varphi$  and  $c$ , using high order Fourier series, as shown in Fig.B1.

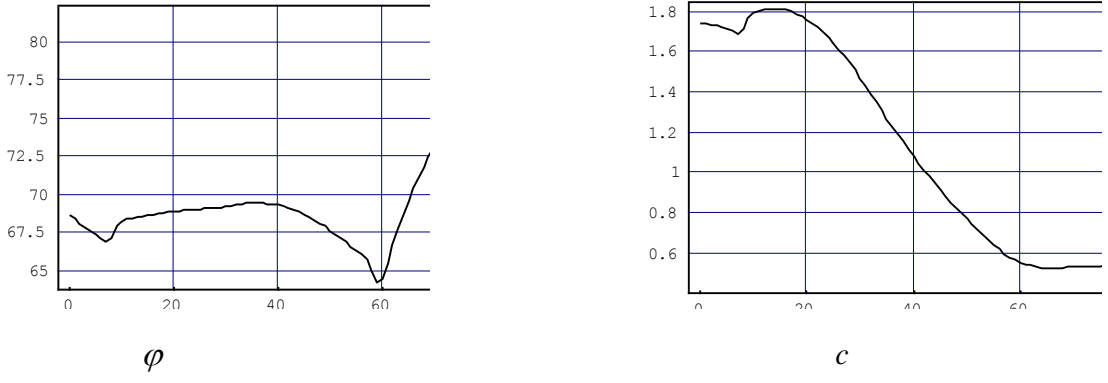
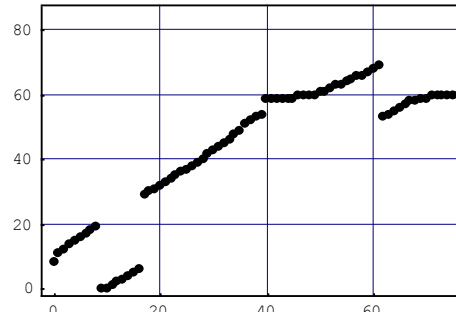
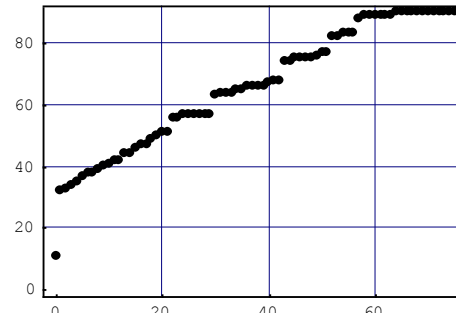


Fig. B1 “Ideal” distributions for  $\varphi$  and  $c$

Implementing these distributions in the failure function in eq. (1) and performing a CPA analysis, the variation of the orientation of failure plane with sample orientation for uniaxial compression and pure shear tests is obtained as follows



(a) Uniaxial compression

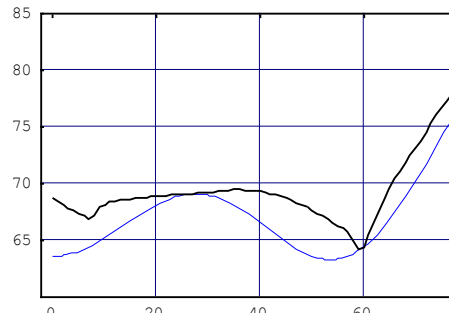


(b) Pure shear

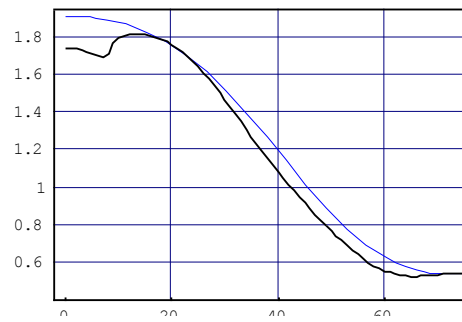
Fig. B2 Variation of failure planes with sample orientation

The figures show that the common failure plane orientations for these two tests are in the range of  $30^0$ - $90^0$ , for which the distribution for  $\varphi$  and  $c$  in eq. (4) can be fitted to the corresponding “ideal” distribution using a constrained optimization approach. The constraints, for the whole range of  $0^0$ - $90^0$ , are given as  $\varphi \leq \varphi_{(ideal)}$  and  $c_{(ideal)} \leq c$ . The resulting distributions of  $\varphi$  and  $c$  are shown in figures B3 and B4 and correspond to the following values of the material constants:

$$\begin{aligned} \Omega_1^\varphi &= 0.078218; & \varphi_1 &= 68.0447; & \varphi_2 &= -742.218; & \varphi_3 &= -10869.2 & (B1) \\ \Omega_1^c &= 0.5; & c_1 &= 1.35854; & c_2 &= -0.135979; & c_3 &= -0.708023 \end{aligned}$$



(a)



(b)

Fig. B3 The distributions of (a)  $\varphi_{(ideal)}$  and  $\varphi$ , (b)  $c_{(ideal)}$  and  $c$